JOURNAL OF STRUCTURAL CONTROL
J. Struct. Control 2002; **00**:1–6 *Prepared using* stcauth.cls *[Version: 2002/11/11 v1.00]*

A model-free method for identification of mass modifications*

Grzegorz Suwała and Łukasz Jankowski*

Smart-Tech Centre, Institute of Fundamental Technological Research, Polish Academy of Sciences, Warsaw, Poland

SUMMARY

In this paper, a model-free methodology for off-line identification of modifications of structural mass is proposed and verified experimentally. The methodology of the virtual distortion method (VDM) is used: the modifications are modeled by the equivalent pseudo-loads that act in the related degrees of freedom of the unmodified structure; their influence on the response is computed using a convolution of the pseudo-loads with the experimentally obtained local impulse-responses. As a result, experimentally measured data is directly used to model the response of the modified structure in a non-parametric way. The approach obviates the need for a parametric numerical model of the structure and for laborious initial updating of its parameters. Moreover, no topological information about the structure is required, besides potential locations of the modifications. The identification is stated as a problem of minimization of the discrepancy between the measured and the modeled responses of the modified structure. The formulation allows the adjoint variable method to be used for a quick first- and second-order sensitivity analysis, so that Hessian-based optimization algorithms can be used for fast convergence. The proposed methodology was experimentally verified using a 3D truss structure with 70 elements. Mass modifications in a single node and in two nodes were considered. Given the initially measured local impulse-responses, a single sensor and a single excitation were sufficient for the identification. Copyright © 2002 John Wiley & Sons, Ltd.

KEY WORDS: mass identification, structural health monitoring (SHM), virtual distortion method (VDM), model-free, non-parametric modeling, adjoint variable method

1. INTRODUCTION

A general motivation for this research is the need for practical identification techniques that could be used in black-box type global monitoring systems for identification of modifications or damage. In general, all existing methods used for structural health monitoring (SHM) can be divided into two groups: local and global approaches. Local approaches are used for precise local identification of small defects in narrow inspection zones and are usually based on ultrasonic testing [1]; they are outside the scope of this paper. Global approaches are used for identification of significant defects in a larger inspection zone, which is often the entire monitored structure. Most of the latter methods, including mass identification methods, can be classified into three general groups [2, 3, 4]:

---

*This is the **pre-peer reviewed version** of the following article: G. Suwała, Ł. Jankowski, A model-free method for identification of mass modifications, *Journal of Structural Control & Health Monitoring*, in press, doi: 10.1002/stc.417, which has been published in final form at `http://dx.doi.org/10.1002/stc.417`.

*Correspondence to: lukasz.jankowski@ippt.gov.pl

Received August 31, 2011

1. *Model-based methods* rely on a parametric numerical model of the monitored structure that is usually a Finite Element (FE) model [5, 6, 7] or a continuum model [8]. The identification is stated in the form of a minimization problem of the discrepancy between the measured response of the modified/damaged structure and the computed response of the modeled structure. Selected parameters of the model, which are assumed to describe the structural modification being identified, are used as the optimization variables.
2. *Pattern recognition methods* rely on a database of numerical fingerprints of low dimension that are extracted from several responses of the modified/damaged structure [9, 10]. The responses used to form the database have to be previously collected either by simulations or by experimental measurements of the structure with introduced modification scenarios, which are to be identified later. The fingerprints should discriminate well between the scenarios. Given the database and the measured response of the involved structure, the actual modification is identified using the fingerprints only, without insight into their actual mechanical meaning, so that neither a numerical model of the structure nor a simulation is required for identification.

Most of these methods can be used for full identification, that is they are capable of detecting, localizing and quantifying the unknown modification or damage. However, in case of many structures, it may not be possible to actually introduce the modifications in order to perform the measurements and build the fingerprint database. Similarly, an accurate numerical model of a complex real-world structure may be hard to obtain and not available [11, 12].

3. Therefore, there is a third group of methods, which rely on certain structural invariants of the monitored structure that can be computed directly from the measured response. These invariants are often modal [3] or based on wavelet or time series analysis [13]. Application possibilities of the response surface methodology is discussed in [14]. In [15], Lyapunov exponents are used for monitoring of a non-linear structure. Modification is detected by assessing the discrepancy between the invariants of the original unmodified structure and these computed from the current measurements. By a proper distribution of sensors in the structure, the invariants can be compared locally, which may allow the detected modification to be also localized.

In a sense, the approach proposed in this paper belongs to the third group, because it avoids actual modifications as well as parametric numerical modeling of the structure; however, it is aimed also at quantification of the modification. The virtual distortion method (VDM) [16, 17, 18] is used, which allows the involved structure to be modeled in an essentially non-parametric way via its locally measured impulse-responses, which are limited to the potential modification points. Modifications of mass are modeled by pseudo-loads that act in the unmodified structure at the modification points. Given the test excitation and the corresponding response of the original unmodified structure, the influence of the modifications is computed by convolving the pseudo-loads with the experimentally obtained impulse-responses. The pseudo-loads are given in the form of a unique solution to a certain linear integral equation, which is discretized into a large and ill-conditioned linear system. The system is structured, so it can be stored in memory in a reduced form and solved using a fast iterative algorithm with regularizing properties; fast matrix-vector multiplication is implemented in frequency domain. Identification of the modifications is formulated as an optimization problem of minimizing the discrepancy between the measured and the modeled structural responses. Fast and exact first- and second-order sensitivity analyses are possible via the adjoint variable method [19, 20, 21]. As a result, quickly convergent Newton optimization algorithms can be directly used. This paper substantially revises and extends the research presented in [22].

The direct problem of modeling the response of the modified structure is stated in the next section. The third section formulates the inverse problem of identification of mass modifications along with its sensitivity analysis. The fourth section discusses discretization and numerical solution of the problem. Experimental results are presented in the last section.

2. RESPONSE OF THE MODIFIED STRUCTURE

In agreement with the general approach of the virtual distortion method (VDM) [16, 17, 18], modifications of structural mass are modeled with pseudo-loads, which are response-coupled and act in the unmodified structure to imitate the inertial effects of the modifications. Hence, the response $\mathbf{u}(t)$ of the modified structure to a given external load $\mathbf{f}(t)$ is expressed as a sum of

1. the response $\mathbf{u}^{\mathrm{L}}(t)$ of the original unmodified structure to the same external load, which is called the *linear response*, and
2. the response $\mathbf{u}^{\mathrm{R}}(t)$ of the same unmodified structure to the pseudo-loads $\mathbf{p}(t)$, which (by an analogy to virtual distortions that model stiffness modifications) is called the *residual response*.

Given the mass modification $\Delta\mathbf{M}$ and the excitation $\mathbf{f}(t)$, the response of the modified structure can be computed using solely characteristics of the original unmodified structure, which can be measured experimentally. The response is found in two steps: first the pseudo-loads are computed and then the corresponding response. The pseudo-loads are response-coupled, hence they are given in an implicit form and have to be found in the first step by solving a certain integral equation.

2.1. Response as a convolution

Let $\mathbf{p}(t)$ be the vector of any loads that excite the original unmodified structure, and denote by $\mathbf{u}^{\mathrm{R}}(t)$ the vector of the corresponding response. It is assumed that the structure is linear and that its equation of motion can be stated as

$$\mathbf{M}\ddot{\mathbf{u}}^{\mathrm{R}}(t) + \mathbf{C}\dot{\mathbf{u}}^{\mathrm{R}}(t) + \mathbf{K}\mathbf{u}^{\mathrm{R}}(t) = \mathbf{p}(t), \tag{1}$$

where $\mathbf{M}$, $\mathbf{C}$ and $\mathbf{K}$ denote respectively the original mass, damping and stiffness matrices. Later in the paper, the excitation $\mathbf{p}(t)$ stands for the pseudo-loads that model the mass modifications, thus the superscript R (residual) is used in the symbol $\mathbf{u}^{\mathrm{R}}(t)$ that denotes the response.

Since Eq. (1) is linear, the response can by expressed in the form of a convolution of the excitation $\mathbf{p}(t)$ with the impulse-response of the structure $\mathbf{B}(t)$,

$$\mathbf{u}^{\mathrm{R}}(t) = \int_0^t \mathbf{B}(t-\tau)\mathbf{p}(\tau)\,d\tau, \tag{2a}$$

$$\ddot{\mathbf{u}}^{\mathrm{R}}(t) = \mathbf{M}^{-1}\mathbf{p}(t) + \int_0^t \ddot{\mathbf{B}}(t-\tau)\mathbf{p}(\tau)\,d\tau. \tag{2b}$$

Notice that the feed-through term $\mathbf{M}^{-1}\mathbf{p}(t)$ that occurs in Eq. (2b) can be included in the impulse-response as an impulsive component at $t = 0$, so that

$$\ddot{\mathbf{u}}^{\mathrm{R}}(t) = \int_0^t \ddot{\mathbf{B}}^{\delta}(t-\tau)\mathbf{p}(\tau)\,d\tau, \tag{3}$$

where

$$\ddot{\mathbf{B}}_{\delta}(t) = \mathbf{M}^{-1}\delta(t) + \ddot{\mathbf{B}}(t), \tag{4}$$

which (although non-standard) seems to be a more practical notation, since the measured impulse-response is the discretized version of $\ddot{\mathbf{B}}_\delta(t)$, see Eq. (22).

2.2. Pseudo-loads

Let $\mathbf{f}(t)$ be the considered external excitation and denote by $\mathbf{u}^{\mathrm{L}}(t)$ the corresponding response of the unmodified structure. The equation of motion can be stated in the following form:

$$\mathbf{M}\ddot{\mathbf{u}}^{\mathrm{L}}(t) + \mathbf{C}\dot{\mathbf{u}}^{\mathrm{L}}(t) + \mathbf{K}\mathbf{u}^{\mathrm{L}}(t) = \mathbf{f}(t). \tag{5}$$

The same test excitation $\mathbf{f}(t)$, when applied to the modified structure, causes the response $\mathbf{u}(t)$. It is described by the following equation of motion:

$$(\mathbf{M} + \Delta\mathbf{M})\,\ddot{\mathbf{u}}(t) + \mathbf{C}\dot{\mathbf{u}}(t) + \mathbf{K}\mathbf{u}(t) = \mathbf{f}(t), \tag{6}$$

where $\Delta\mathbf{M}$ stands for the mass modification and where it is assumed that the environmental damping is not considerably influenced by the modification. Equation (6) can be rearranged into the following form:

$$\mathbf{M}\ddot{\mathbf{u}}(t) + \mathbf{C}\dot{\mathbf{u}}(t) + \mathbf{K}\mathbf{u}(t) = \mathbf{f}(t) + \mathbf{p}(t), \tag{7}$$

which is in fact the equation of motion of the unmodified structure, where the mass modification $\Delta\mathbf{M}$ is modeled by the pseudo-load $\mathbf{p}(t)$,

$$\mathbf{p}(t) = -\Delta\mathbf{M}\ddot{\mathbf{u}}(t). \tag{8}$$

Notice that Eq. (8) states the pseudo-load in an implicit way, as the response $\mathbf{u}(t)$ obviously depends also on the pseudo-load $\mathbf{p}(t)$, besides the excitation $\mathbf{f}(t)$. The structure is linear, and hence, according to Eqs. (1), (5) and (7), the response $\mathbf{u}(t)$ is the sum of the responses $\mathbf{u}^{\mathrm{L}}(t)$ and $\mathbf{u}^{\mathrm{R}}(t)$,

$$\mathbf{u}(t) = \mathbf{u}^{\mathrm{L}}(t) + \mathbf{u}^{\mathrm{R}}(t). \tag{9}$$

Equations (9), (8) and (2b) yield together

$$\left[\mathbf{I} + \Delta\mathbf{M}\mathbf{M}^{-1}\right]\mathbf{p}(t) + \Delta\mathbf{M}\int_0^t \ddot{\mathbf{B}}(t-\tau)\mathbf{p}(\tau)\,d\tau = -\Delta\mathbf{M}\ddot{\mathbf{u}}^{\mathrm{L}}(t), \tag{10a}$$

which is a system of Volterra integral equations of the second kind with the pseudo-loads $\mathbf{p}(t)$ as the unknowns. Even though such a system is usually very ill-conditioned, it follows from the Riesz theory [23] that it is well-posed, provided the matrix $\mathbf{I}+\Delta\mathbf{M}\mathbf{M}^{-1}$ is non-singular, which is equivalent to the non-singularity of $\mathbf{M}+\Delta\mathbf{M}$. Therefore, Eq. (10a) has a unique solution, if the considered mass modification is not negative enough to delete a part of the structure. Equation (10a) can be also stated using Eq. (4) in the following form:

$$\mathbf{p}(t) + \Delta\mathbf{M}\int_0^t \ddot{\mathbf{B}}_\delta(t-\tau)\mathbf{p}(\tau)\,d\tau = -\Delta\mathbf{M}\ddot{\mathbf{u}}^{\mathrm{L}}(t), \tag{10b}$$

which uses the experimentally measurable impulse-response $\ddot{\mathbf{B}}_\delta(t)$ and does not involve the unknown mass matrix $\mathbf{M}$.

2.3. Response of the modified structure

Mass modifications are modeled by pseudo-loads $\mathbf{p}(t)$ that act in the original unmodified structure in the degrees of freedom (DOFs) that are related to the modification. For a given modification $\Delta\mathbf{M}$ and excitation $\mathbf{f}(t)$, the corresponding pseudo-loads can be obtained by solving the system Eq. (10b). Then, the response of the modified structure to $\mathbf{f}(t)$ can be computed using Eqs. (9) and (2a) as a sum of the response of the unmodified structure and the cumulative effects of the pseudo-loads,

$$\mathbf{u}(t) = \mathbf{u}^{\mathrm{L}}(t) + \int_0^t \mathbf{B}(t-\tau)\mathbf{p}(\tau)\,d\tau, \tag{11}$$

where $\mathbf{B}(t)$ is the matrix of the impulse-response functions of the original unmodified structure.

2.4. Computations and required data

For a given modification $\Delta\mathbf{M}$ and excitation $\mathbf{f}(t)$, the response of the modified structure is computed in two steps:

1. the pseudo-loads that model the mass modifications are found by solving Eq. (10b);
2. the response is computed by Eq. (11).

Computations in both steps require, besides $\Delta\mathbf{M}$, solely the characteristics of the unmodified structure. These are:

- the responses $\mathbf{u}^{\mathrm{L}}(t)$ and $\ddot{\mathbf{u}}^{\mathrm{L}}(t)$ to the considered excitation $\mathbf{f}(t)$;
- the matrices of the impulse-responses $\mathbf{B}(t)$ and $\ddot{\mathbf{B}}_{\delta}(t)$.

All these characteristics can be measured experimentally prior to modeling of the modifications, so that there is no need to build and update a parametric numerical model of neither the unmodified nor the modified structure. According to Eq. (8), the pseudo-loads vanish in the DOFs that are unrelated to the mass modification $\Delta\mathbf{M}$. As a result, the response $\ddot{\mathbf{u}}^{\mathrm{L}}(t)$ and the impulse-responses $\mathbf{B}(t)$ and $\ddot{\mathbf{B}}_{\delta}(t)$ can be restricted to the DOFs that are related to the mass modifications, which makes the experimental measurements more feasible.

3. IDENTIFICATION OF MODIFICATIONS

The inverse problem is stated here in the standard form of a problem of minimization of the objective function, which is the mean square discrepancy between the measured and the modeled responses of the modified structure to a certain test excitation. A fast and exact first- and second-order sensitivity analysis is proposed. The method of adjoint variable is used, which is faster by one order of magnitude in comparison to the direct differentiation method [19, 20, 21]. As a result, exact Newton optimization methods can be used for fast convergence of the optimization [24].

3.1. Objective function

Given the test excitation $\mathbf{f}(t)$, the identification of the unknown mass modification is based on the comparison between the measured response of the modified structure $\mathbf{u}^{\mathrm{M}}(t)$ and the modeled response $\mathbf{u}(t)$. The following objective function is used:

$$F(\Delta\mathbf{M}) = \frac{1}{2}\int_0^T \|\mathbf{d}(t)\|^2\,dt, \tag{12a}$$

where

$$\mathbf{d}(t) = \mathbf{u}^{\mathrm{M}}(t) - \mathbf{u}(t). \tag{12b}$$

The identification amounts to the minimization of the function F with respect to a chosen set of parameters that define the mass modification $\Delta\mathbf{M}$ and influence the modeled response $\mathbf{u}(t)$.

3.2. First-order sensitivity analysis

Direct differentiations of the objective function Eq. (12a) and of the response Eq. (11) with respect to the ith parameter of mass modification yield the following formula:

$$F_i(\Delta\mathbf{M}) = -\int_0^T \mathbf{d}^{\mathrm{T}}(t)\,\mathbf{u}_i(t)\,dt, \tag{13a}$$

where

$$\mathbf{u}_i(t) = \int_0^t \mathbf{B}(t-\tau)\mathbf{p}_i(\tau)\,d\tau. \tag{13b}$$

Equations (13) involve derivatives of the pseudo-loads $\mathbf{p}_i(t)$. The direct method of sensitivity analysis (direct differentiation method) computes them using the differentiated Eq. (10b),

$$\mathbf{p}_i(t) + \Delta\mathbf{M}\int_0^t \ddot{\mathbf{B}}_\delta(t-\tau)\mathbf{p}_i(\tau)\,d\tau = -\Delta\mathbf{M}_i\ddot{\mathbf{u}}(t), \tag{14}$$

which has to be solved several times, separately for each i.

However, there is a much quicker way that makes use of the method of adjoint variable. First, the scalar product of Eq. (14) and a vector $\boldsymbol{\lambda}(t)$ of adjoint variables is integrated with respect to time and the result is added to Eq. (13a). Then, the order of integration is reversed and all the terms containing $\mathbf{p}_i(t)$ are collected together to yield

$$\begin{aligned} F_i(\Delta\mathbf{M}) = &\int_0^T \left[\boldsymbol{\lambda}^{\mathrm{T}}(t) + \int_t^T \boldsymbol{\lambda}(\tau)^{\mathrm{T}}\Delta\mathbf{M}\ddot{\mathbf{B}}_\delta(\tau-t)\,d\tau - \int_t^T \mathbf{d}^{\mathrm{T}}(\tau)\mathbf{B}(\tau-t)d\tau\right]\mathbf{p}_i(t)\,dt \\ &+ \int_0^T \boldsymbol{\lambda}^{\mathrm{T}}(t)\Delta\mathbf{M}_i\ddot{\mathbf{u}}(t)\,dt \end{aligned} \tag{15}$$

The vector $\boldsymbol{\lambda}(t)$ of the adjoint variables is chosen in such a way that in Eq. (15) the multiplier term of $\mathbf{p}_i(t)$ vanishes. It happens if $\boldsymbol{\lambda}(t)$ is a solution to

$$\boldsymbol{\lambda}(t) + \int_t^T \ddot{\mathbf{B}}_\delta^{\mathrm{T}}(\tau-t)\Delta\mathbf{M}\boldsymbol{\lambda}(\tau)\,d\tau = \int_t^T \mathbf{B}^{\mathrm{T}}(\tau-t)\mathbf{d}(t)\,d\tau, \tag{16}$$

which is called the adjoint integral equation and can be also stated in the standard form using $\mathbf{B}(t)$, as in Eq. (10a). Equation (16), as Eqs. (10), is a Volterra integral equation of the second kind, so it always has a unique solution, provided that $\mathbf{M} + \Delta\mathbf{M}$ is non-singular. Finally, given the adjoint variable, the derivatives of the pseudo-loads in Eq. (15) vanish and the derivative $F_i(\Delta\mathbf{M})$ of the objective function can be computed simply as

$$F_i(\Delta\mathbf{M}) = \int_0^T \boldsymbol{\lambda}^{\mathrm{T}}(t)\Delta\mathbf{M}_i\ddot{\mathbf{u}}(t)\,dt. \tag{17}$$

Notice that the adjoint variable $\boldsymbol{\lambda}(t)$ is independent of i, hence the gradient of the objective function $\nabla F(\Delta\mathbf{M})$ can be computed at the cost of only a single solution of the adjoint integral equation, instead of multiple solutions of Eq. (14), which is required by the direct differentiation method.

3.3. Second-order sensitivity analysis

Direct differentiation of Eqs. (13) with respect to the jth parameter of mass modification yields

$$F_{ij}(\Delta\mathbf{M}) = \int_0^T \mathbf{u}_j^{\mathrm{T}}(t)\,\mathbf{u}_i(t)\,dt - \int_0^T \mathbf{d}^{\mathrm{T}}(t)\,\mathbf{u}_{ij}(t)\,dt, \tag{18a}$$

where

$$\mathbf{u}_{ij}(t) = \int_0^t \mathbf{B}(t-\tau)\mathbf{p}_{ij}(\tau)\,d\tau, \tag{18b}$$

which contains the first and the second derivatives of the pseudo-loads. The direct differentiation method computes $\mathbf{p}_{ij}(t)$ using the differentiated Eq. (14),

$$\mathbf{p}_{ij}(t) + \Delta\mathbf{M}\int_0^t \ddot{\mathbf{B}}_\delta(t-\tau)\mathbf{p}_{ij}(\tau)\,d\tau = -\Delta\mathbf{M}_i\ddot{\mathbf{u}}_j(t) - \Delta\mathbf{M}_j\ddot{\mathbf{u}}_i(t), \tag{19}$$

where it is assumed that $\Delta\mathbf{M}$ is a linear function of the mass modification parameters (that is $\Delta\mathbf{M}_{ij} = \mathbf{0}$) and which has to be solved several times, separately for each element of the Hessian.

The direct-adjoint method, which seems to be the quickest from the family of the second-order adjoint variable methods [21], can reduce the numerical costs by one order of magnitude. In the same way as in the first-order analysis, a scalar product of the adjoint vector and Eq. (19) is integrated with respect to time and the result is added to Eq. (18a) in order to eliminate the second derivatives of the pseudo-loads. As a result, a considerably simpler formula for the element $F_{ij}(\Delta\mathbf{M})$ of the Hessian is obtained:

$$F_{ij}(\Delta\mathbf{M}) = \int_0^T \mathbf{u}_i(t)\,\mathbf{u}_j(t)\,dt + \int_0^T \boldsymbol{\lambda}^{\mathrm{T}}(t)\Delta\mathbf{M}_i\ddot{\mathbf{u}}_j(t)\,dt + \int_0^T \boldsymbol{\lambda}^{\mathrm{T}}(t)\Delta\mathbf{M}_j\ddot{\mathbf{u}}_i(t)\,dt, \tag{20}$$

where

$$\ddot{\mathbf{u}}_i(t) = \int_0^t \ddot{\mathbf{B}}_\delta(t-\tau)\mathbf{p}_i(\tau)\,d\tau \tag{21}$$

and the first derivatives of the pseudo-load $\mathbf{p}_i(t)$ have to be obtained using the direct differentiation method, that is by solving Eq. (14) separately for each mass modification parameter i.

Note that, if the second-order analysis is performed and $\mathbf{u}_i(t)$ and $\mathbf{p}_i(t)$ are known, the gradient of the objective function can be computed at a low cost using Eq. (13a) and compared to that obtained from Eq. (17) for verification purposes.

3.4. Required data

The inverse problem is solved via an iterative optimization procedure. In its each step, the objective function has to be computed, possibly along with the gradient and the Hessian. The following purely experimental data are required:

- the measured response $\mathbf{u}^{\mathrm{M}}(t)$ of the modified structure to a certain reproducible test excitation $\mathbf{f}(t)$;
- the measured responses $\mathbf{u}^{\mathrm{L}}(t)$ and $\ddot{\mathbf{u}}^{\mathrm{L}}(t)$ of the original unmodified structure to the same test excitation $\mathbf{f}(t)$;
- the matrices of the impulse-responses $\mathbf{B}(t)$ and $\ddot{\mathbf{B}}_\delta(t)$ of the original unmodified structure.

As in the case of the direct problem, the response $\ddot{\mathbf{u}}^{\mathrm{L}}(t)$ and the impulse-responses are restricted to the DOFs that are related to the potential mass modifications.

4. DISCRETIZATION AND NUMERICAL SOLUTION

4.1. Discretization of the direct problem

The proposed approach is model-free and thus intended for practical implementations. In practice, all data are experimentally measured. Therefore, all the required responses, instead of being continuous, are vectors that are sampled in discrete time points every Δt. In particular, the measured impulse-responses, which are denoted here by $\mathbf{D}(t)$ and $\ddot{\mathbf{D}}(t)$, are the discrete responses to one-time-step unit excitations, so that

$$\mathbf{D}(t) \approx \mathbf{B}(t)\Delta t, \qquad \ddot{\mathbf{D}}(t) \approx \begin{cases} \mathbf{M}^{-1} + \ddot{\mathbf{B}}(0)\Delta t & \text{if } t = 0, \\ \ddot{\mathbf{B}}(t)\Delta t & \text{otherwise,} \end{cases} \tag{22}$$

where the impulsive component of $\ddot{\mathbf{B}}_\delta(t)$ is included in $\ddot{\mathbf{D}}(0)$, compare to Eq. (4).

As a result, the continuous integral equation Eq. (10b) is transformed into the following discrete linear system:

$$\sum_{\tau=0}^{t} \left[\Delta\mathbf{M}\ddot{\mathbf{D}}(t-\tau) + \delta_{\tau t}\mathbf{I}\right] \mathbf{p}(\tau) = -\Delta\mathbf{M}\ddot{\mathbf{u}}^{\mathrm{L}}(t), \tag{23}$$

where $\mathbf{I}$ is the identity matrix of appropriate dimensions and $\delta_{\tau t}$ denotes Kronecker's delta. Equation (23) can be collected for all considered time steps t and stated in the form of a single large linear system

$$\mathbf{A}\mathbf{p} = -\Delta\mathbf{M}\ddot{\mathbf{u}}^{\mathrm{L}}, \tag{24}$$

where the vectors $\mathbf{p}$ and $\ddot{\mathbf{u}}^{\mathrm{L}}$ collect the pseudo-loads and the acceleration responses of the unmodified structure for all DOFs related to mass modifications and in all time steps. The system matrix $\mathbf{A}$ is a $3n \times 3n$ block matrix with $T \times T$ lower triangular Teoplitz blocks, where T is the number of time steps and n is the number of the nodes related to mass modifications. The structure of a typical system matrix is illustrated in Figure 5. Equation (24) is solved to obtain the discrete pseudo-loads $\mathbf{p}$; the modeled discrete responses of the modified structure can be then computed as

$$\mathbf{u} = \mathbf{u}^{\mathrm{L}} + \mathbf{D}\mathbf{p}, \qquad \ddot{\mathbf{u}} = \ddot{\mathbf{u}}^{\mathrm{L}} + \ddot{\mathbf{D}}\mathbf{p}, \tag{25}$$

where the matrices $\mathbf{D}$ and $\ddot{\mathbf{D}}$ are block matrices with Toeplitz blocks that are the discrete counterparts of the integral operators in Eqs. (2).

4.2. Discretization of the inverse problem and sensitivity analysis

Identification of mass modifications amounts to the minimization of the following objective function:

$$F(\Delta\mathbf{M}) = \frac{1}{2}\mathbf{d}^{\mathrm{T}}\mathbf{d}, \tag{26a}$$

where

$$\mathbf{d} = \mathbf{u}^{\mathrm{M}} - \mathbf{u}. \tag{26b}$$

and the vector $\mathbf{u}^{\mathrm{M}}$ denotes the measured response of the modified structure collected for all the considered sensors in all time steps. The derivative $F_i(\Delta\mathbf{M})$ of the objective function can be computed by collecting for all time steps the discrete versions of Eqs. (17) and (16):

$$F_i(\Delta\mathbf{M}) = \boldsymbol{\lambda}^{\mathrm{T}}\Delta\mathbf{M}_i\ddot{\mathbf{u}}, \tag{27}$$

Table I. Computations required for a first-order and a second-order sensitivity analysis. It is assumed that $\mathbf{D}$, $\ddot{\mathbf{D}}$, $\mathbf{u}^{\mathrm{M}}$ and $\mathbf{u}^{\mathrm{L}}$ are known

no.	1st order	2nd order	computation	formula
1.	×	×	system matrix $\mathbf{A}$	Eq. (23)
2.	×	×	pseudo-loads $\mathbf{p}$	Eq. (24)
3.	×	×	modeled responses $\mathbf{u}$ and $\ddot{\mathbf{u}}$	Eq. (25)
4.	×	×	residual vector $\mathbf{d}$	Eq. (26b)
5.	×	×	objective function $F(\Delta\mathbf{M})$	Eq. (26a)
6.	×	×	discrete adjoint variables $\boldsymbol{\lambda}$	Eq. (28)
7.		×	derivatives of the pseudo-loads $\mathbf{p}_i$ (for all i)	Eq. (31)
8a.	×	×	gradient of the objective function $\nabla F(\Delta\mathbf{M})$	Eq. (27)
8b		×	gradient of the objective function $\nabla F(\Delta\mathbf{M})$	Eq. (32)
9.		×	Hessian of the objective function	Eq. (29)

where the vector $\boldsymbol{\lambda}$ collects the discrete adjoint variables that can be obtained at the cost of a single solution of the discrete adjoint equation

$$\mathbf{A}^{\mathrm{T}}\boldsymbol{\lambda} = \mathbf{B}^{\mathrm{T}}\mathbf{d}, \tag{28}$$

which is the discrete counterpart of the continuous adjoint integral equation Eq. (16). In a similar way, the Hessian of the objective function can be computed as

$$F_{ij}(\Delta\mathbf{M}) = \mathbf{u}_i^{\mathrm{T}}\,\mathbf{u}_j + \boldsymbol{\lambda}^{\mathrm{T}}\Delta\mathbf{M}_i\ddot{\mathbf{u}}_j + \boldsymbol{\lambda}^{\mathrm{T}}\Delta\mathbf{M}_j\ddot{\mathbf{u}}_i, \tag{29}$$

where

$$\mathbf{u}_i = \mathbf{D}\mathbf{p}_i, \qquad \ddot{\mathbf{u}}_i = \ddot{\mathbf{D}}\mathbf{p}_i, \tag{30}$$

and the vector $\mathbf{p}_i$ of the first-order derivatives of the pseudo-loads has to be obtained by solving the discrete counterpart of Eq. (14),

$$\mathbf{A}\mathbf{p}_i = -\Delta\mathbf{M}_i\ddot{\mathbf{u}}, \tag{31}$$

separately for each i, that is for each parameter of mass modification. As in Eq. (20), it is assumed in Eq. (29) that $\Delta\mathbf{M}_{ij}$ vanish, which happens for example if the modification parameters are simply the added/removed masses, as it is usually the case in practice. The time complexity of Hessian computation is linear with respect to the number of the considered parameters of modification, instead of the quadratic complexity of the direct method. Notice that the second-order sensitivity analysis requires computation of $\mathbf{u}_i$, which can be then used in the discrete counterpart of Eq. (13a),

$$F_i(\Delta\mathbf{M}) = -\mathbf{u}_i^{\mathrm{T}}\,\mathbf{d}, \tag{32}$$

for a low-cost verification of the gradients obtained via Eq. (27).

Given the structure-specific impulse-responses $\mathbf{D}$ and $\ddot{\mathbf{D}}$, as well as the responses to the test excitations, $\mathbf{u}^{\mathrm{M}}$ and $\mathbf{u}^{\mathrm{L}}$, the computations required for a first-order and a second-order sensitivity analysis are summarized in Table I.

4.3. Numerical remarks

Theoretically, given the discrete versions of the direct and the inverse problems, identification of mass modifications is straightforward: it amounts to an iterative minimization of the objective function. In each iteration, a sensitivity analysis is performed, see Table I. Two square linear systems have to be solved to obtain $\mathbf{p}$ and $\boldsymbol{\lambda}$ (Eqs. (24) and (28)); if a second-order optimization method is used, then also all $\mathbf{p}_i$ have to be computed by solving Eq. (31) separately for each optimization variable. In all cases, the system matrix is $\mathbf{A}$ or $\mathbf{A}^{\mathrm{T}}$. However, all responses are stored and processed in time domain, which can result in large dimensions of $\mathbf{A}$. It is a danse $3n \times 3n$ block matrix with $T \times T$ blocks, where T is the number of time steps and n is the number of the nodes related to mass modifications; the total dimensions are thus $3nT \times 3nT$. In case of a longer time interval or a non-localized modification, the matrix can become huge and unmanageable by standard numerical techniques. Moreover, as can be expected from the Toeplitz structure of its blocks [25], the matrix is significantly ill-conditioned, and a regularization technique has to be used in order to obtain meaningful solutions. It is proposed here to use the fast iterative algorithm of conjugate gradient least squares (CGLS) [26] to solve the involved systems, since

- the CGLS method has good regularizing properties. The number of iterations plays the role of the regularization parameter: the more iterations, the more exact but less regularized (that is more influenced by the measurement error) is the solution;
- the method uses the system matrix $\mathbf{A}$ only in the form of the matrix-vector products $\mathbf{Ax}$ and $\mathbf{A}^{\mathrm{T}}\mathbf{y}$, so that no costly matrix decomposition and even no direct access to its elements are necessary. In fact, two black-box procedures implementing the respective multiplications are enough.

Moreover, the block Toeplits structure of the system matrix $\mathbf{A}$ can be also exploited:

- Each block of $\mathbf{A}$ is a $T \times T$ lower triangular Toeplitz block, hence it can be stored in computer memory in a reduced form using only T elements instead of T^2.
- In the CGLS method, the system matrix $\mathbf{A}$ is present only implicitly in the form of matrix-vector products. For each of the $T \times T$ Toeplitz block, the product can be computed in frequency domain using the FFT in time $O(T \log T)$ instead of $O(T^2)$.

5. EXPERIMENTAL VERIFICATION

5.1. The structure

A 3D truss structure with 26 nodes and 70 elements was used in the experimental verification, see Figure 1. The structure was 4 m long, and the elements were circular steel tubes with the radius of 22 mm, the thickness of 1 mm and the lengths of 500 mm or 707 mm; the total weight was approximately 32 kg. The right-hand side nodes were free to move in the longitudinal direction only, while the two opposite left-hand side nodes were turned into fixed supports.

Only nodal mass modifications were considered. They were realized by fixing concentrated masses at one or two of the nodes marked M_1, M_2 and M_3 in Figure 1; the location of the modifications was assumed to be known. Two modification scenarios were investigated:

1. modification of a single nodal mass in M_1, M_2 or M_3,
2. modification of two nodal masses in the nodes M_1 and M_3.

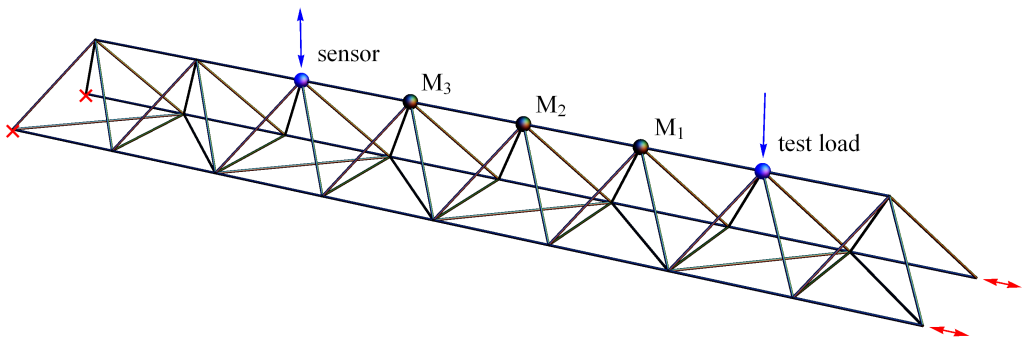

Figure 1. Truss structure used in the experimental verification

5.2. *Excitations and measurements*

Figure 1 shows the location of the test excitation $\mathbf{f}$ and the single sensor that was used to measure $\mathbf{u}^{\mathrm{L}}$ and $\mathbf{u}^{\mathrm{M}}$. A modal hammer was used to generate the test excitation $\mathbf{f}$, as well as the excitations used in measurements of the necessary impulse-responses. Only accelerometers were used; the signals were collected by a Brüel & Kjær PULSE system, sampled at 65.5 kHz and transferred to a desktop PC for further analysis. The acquisition system internally double-integrated the acceleration responses to obtain the displacements. In each case, four responses have been recorded; their mean was used in further computations in order to diminish the effects of the measurement noise. For each response, a total of $15\,000$ time steps was recorded, which corresponds approximately to 230 ms or 7.2 periods of the first natural vibration (31.5 Hz). In the case of two nodal mass modifications, the matrix $\mathbf{A}$ in Eq. (24) is thus a 6×6 block matrix with the total dimensions of $90\,000 \times 90\,000$. The matrix is dense, and if stored in the full form using standard 8-byte double floating point numbers, it would require as much as 60.3 GB of storage. On the other hand, exploitation of the Toeplitz block structure allowed the matrix to be stored in 4.1 MB only.

Notice that the discrete impulse-responses $\mathbf{D}(t)$ and $\ddot{\mathbf{D}}(t)$ are the responses to a one-time-step unit excitations, while the modal hammer generates excitations that last several time steps. Therefore, the mean recorded responses $\mathbf{D}^{\text{measured}}(t)$ and $\ddot{\mathbf{D}}^{\text{measured}}(t)$ had to be deconvoluted with respect to the mean measured hammer excitation $\mathbf{f}^{\text{hammer}}(t)$ by solving a number of large linear systems of the following Toeplitz form:

$$\sum_{\tau=0}^{t} f_j^{\text{hammer}}(t-\tau) D_{ij}(\tau) = D_{ij}^{\text{measured}}(t),$$

where i and j index respectively the measurement and the excitation DOFs. The deconvolutions were performed iteratively using the CGLS method, as described in Section 4.3.

5.3. *Single nodal mass modification*

In the first considered scenario, a single mass modification occurred in one of the nodes M_1, M_2 or M_3; the location was assumed to be known. Four different masses of 1.36 kg, 2.86 kg, 3.86 kg and 5.36 kg were used in each of the three nodes; in comparison to the total mass of the original structure (32 kg),

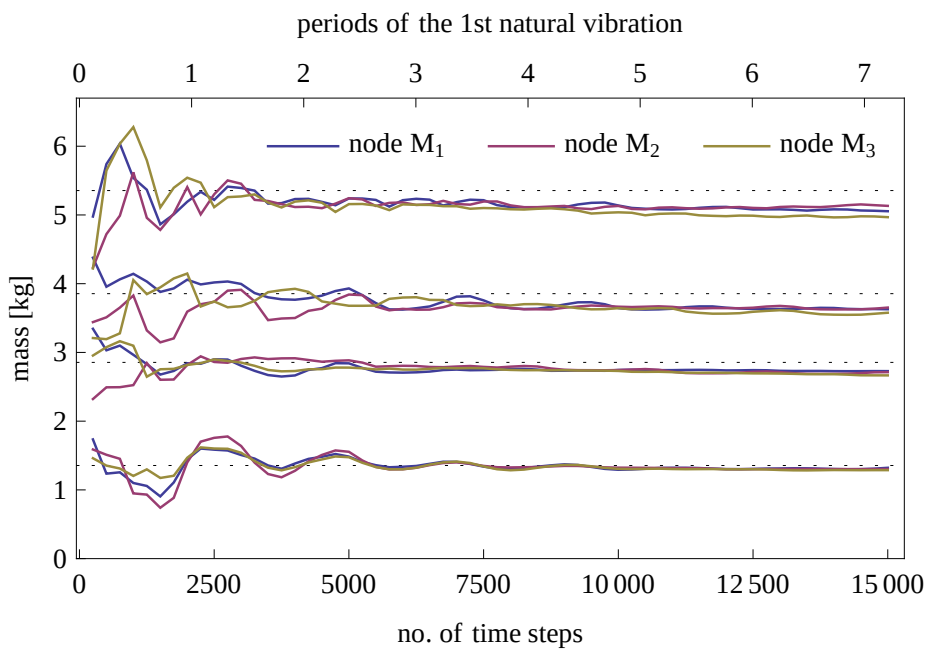

Figure 2. Single nodal mass modification: identification results in dependence on the considered length of the responses; the dotted lines mark the actual modifications

they corresponded to the relative mass modifications between 4.25% and 16.75%. In all identifications, the Newton optimization algorithm with the exact second derivatives was used. In each optimization step, the ill-conditioned systems Eqs. (24), (28) and (31) were solved iteratively using 1000 CGLS iterations, which allowed the computed responses to stabilize before being overly influenced by the measurement errors.

The stability of the identification procedure was tested with respect to the length of the responses. All the identifications were repeatedly performed using the lengths from 250 up to all 15000 time steps (3.8 ms to 292 ms). The results are plotted in Figure 2. At short response lengths, the identification results were strongly dependent on the number of time steps used; it was thus assumed that at least 7500 time steps (115 ms or 3.6 periods of the first natural vibration) were necessary for stable results. In general, the identification results underestimated the modifications; the relative identification errors ranged between -8% and 1% with the mean of -4.6%. Figure 3 plots in the logarithmic scale the objective functions computed using 15000 time steps for all the four masses and the three nodes; the minima are clearly distinguishable. As an example, Figure 4 compares the three full-length responses that correspond to the best-fitting case of mass 2.86 kg in the node M_3 (identified mass 2.67 kg). The difference between $\mathbf{u}^{\mathrm{L}}$ and $\mathbf{u}^{\mathrm{M}}$, that is the influence of the added mass on the measured response is clear.

5.4. Modification of two nodal masses

In the second considered scenario, two nodal masses are modified simultaneously in two nodes of the structure (M_1 and M_3). Six different cases have been tested, that is all the six possible combinations of

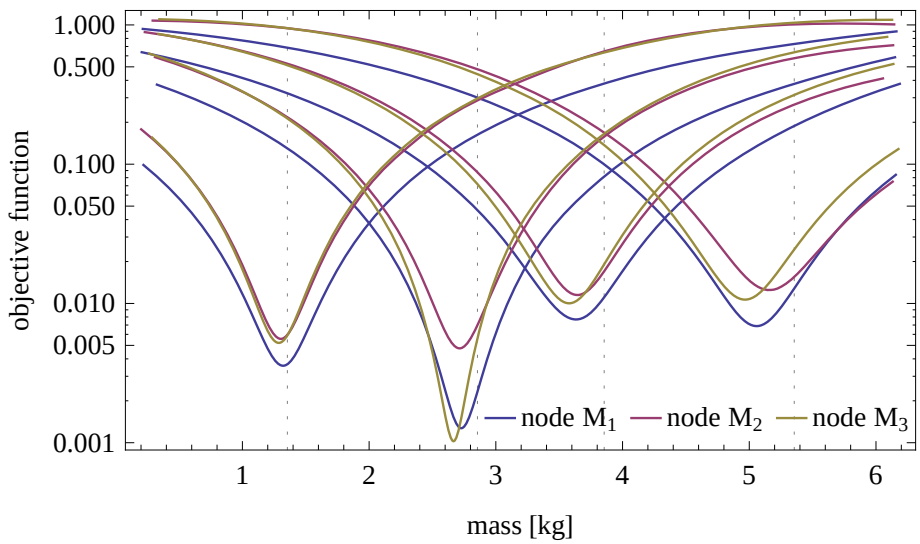

Figure 3. Single nodal mass modification: objective functions computed using 15000 time steps for all three nodes and four tested masses

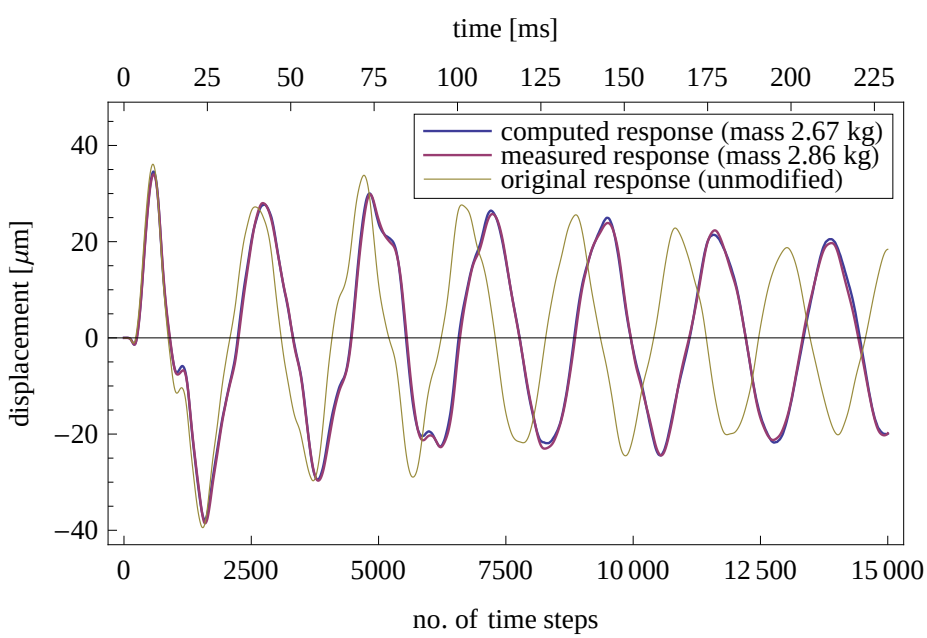

Figure 4. Single nodal mass modification (node M_3, actual mass 2.86 kg, identified mass 2.67 kg): the computed response $\mathbf{u}$ and the measured responses $\mathbf{u}^M$, $\mathbf{u}^L$ of the modified and the original structures

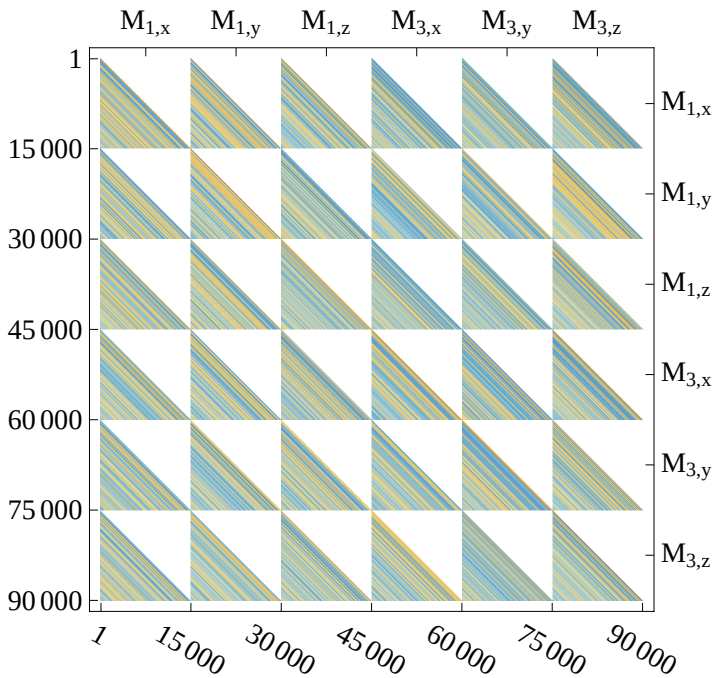

Figure 5. Modification of two nodal masses: structure of the system matrix $\mathbf{A}$ in Eq. (24)

$\mathrm{M}_1 \in \{1.36\,\mathrm{kg}, 2.86\,\mathrm{kg}\}$ and $\mathrm{M}_3 \in \{1.39\,\mathrm{kg}, 2.89\,\mathrm{kg}, 3.89\,\mathrm{kg}\}$. The system matrix $\mathbf{A}$ in Eq. (24) is a 6×6 Toeplitz block matrix, where each block row and block column corresponds to one of the six DOFs of the two considered nodes. For the full-length responses (15000 time steps), its total dimensions are 90000×90000; the structure of such a matrix is illustrated in Figure 5. In order to test the stability of the results, all the identifications have been performed repeatedly using the responses of different lengths: each 250 time steps in the range from 7500 to 15000 time steps.

Figure 6 shows the results of the identifications, which have been obtained using a modified Newton optimization algorithm and exact Hessians. The relative identification errors were higher than in the case of a single nodal mass modification, which was the result of the significant ill-conditioning of the identification problem. As an example, Figure 7 plots the contours of (the logarithm of) the objective function that corresponds to the actual mass modifications $(\mathrm{M}_1, \mathrm{M}_3) = (2.86\,\mathrm{kg}, 1.39\,\mathrm{kg})$ and was computed using all 15000 time steps. The minimum was found at $(3.05\,\mathrm{kg}, 1.07\,\mathrm{kg})$, and the relative identification errors were $(7\%, 23\%)$. A high degree of ill-conditioning is apparent in the shape of the objective function, which formed a long and narrow valley. As a result, it was relatively easy to find the bottom line of the valley (which corresponded approximately to the constant sum of the two modifications), while the exact location of the minimum along the bottom line was sensitive to measurement errors and varied for different numbers of time steps. The degree of ill-conditioning can be quantized by the condition number of the Hessian at the minimum; it was computed to be approximately 500. Figure 8 compares the three responses related to the considered case: the measured response of the original unmodified structure, the measured response of the modified structure and the response modeled for the identified mass modifications.

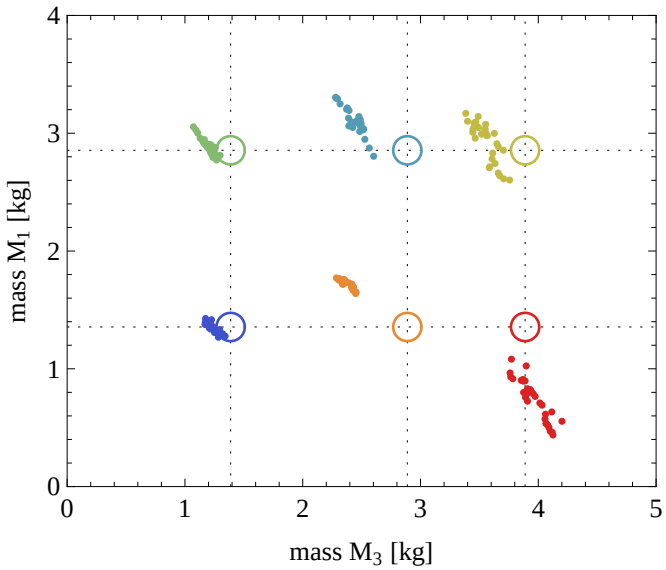

Figure 6. Modification of two nodal masses: identification results for different considered lengths of the responses. The circles mark the actual modifications, the dots mark the identification results for different considered numbers of time steps (7500 to 15000)

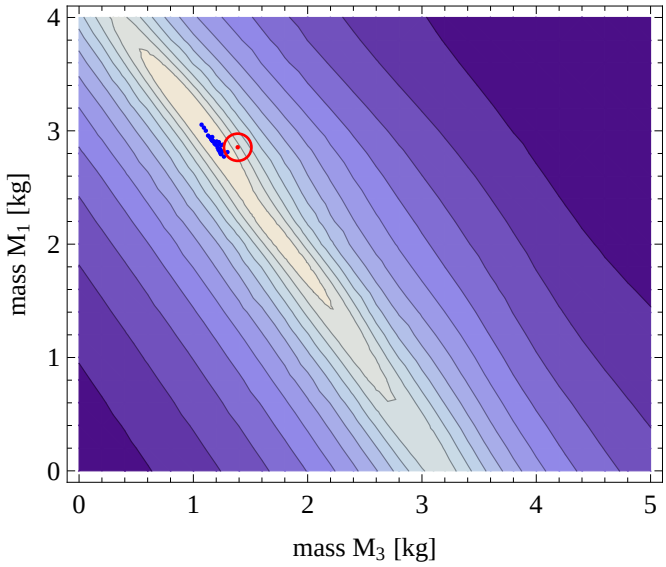

Figure 7. Modification of two nodal masses: contours of (the logarithm of) the objective function computed for the actual modifications $M_1 = 1.36\,\text{kg}$ and $M_3 = 2.89\,\text{kg}$. The center of the circle marks the actual modification, the dots mark the identification results obtained for different considered numbers of time steps (7500 to 15000)

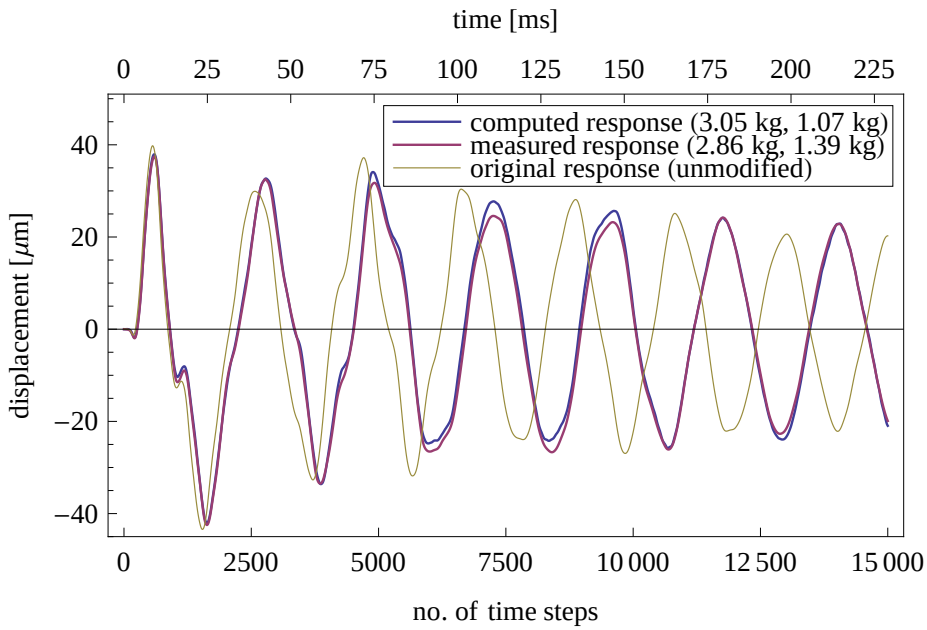

Figure 8. Modification of two nodal masses (M_1,M_3): measured response at the actual masses (2.86 kg, 1.39 kg), modeled response for the identified masses (3.05 kg, 1.07 kg) and the response of the original unmodified structure

6. CONCLUSIONS

This paper proposes a model-free approach to identification of modifications of structural mass. The approach is based on the virtual distortion method (VDM) and requires neither parametric numerical model of the monitored structure nor any topological information, besides the locations of the potential modifications. Experimentally measured local impulse-responses are directly used to model the response of the modified structure in an essentially non-parametric way.

A 70-element 3D truss structure was used in the experimental validation. Modifications of one and two nodal masses were identified using a single impact test excitation and a single test sensor. The average relative errors of identification of single modifications were less than 5%. The errors were larger in the cases of two modifications, which was a result of the ill-conditioning of the problem. The accuracy depends on the characteristics, number and placement of the test excitations and test sensors. The limiting resolution of the identification is a subject of further research and a topic of an upcoming paper. The approach will be generalized to model-free identification of structural damages and dynamic excitations.

ACKNOWLEDGEMENTS

The authors gratefully acknowledge the support through the Foundation for Polish Science TEAM Programme 'Smart&Safe' co-financed by the EU European Regional Development Fund. Financial support of Structural Funds in the Operational Programme – Innovative Economy (IE OP) financed from the European Regional Development Fund – Project No POIG.0101.02-00-015/08 (PKAERO) is gratefully acknowledged.

REFERENCES

1. Staszewski WJ. Structural Engineering Structural Health Monitoring using Guided Ultrasonic Waves. In *Advances in Smart Technologies,* Holnicki-Szulc J, Soares CAM (eds). Springer, 2003; 117-162.
2. Fritzen CP, Kraemer P. Self-diagnosis of smart structures based on dynamical properties. *Mechanical Systems and Signal Processing* 2009; **23**(6):1830–1845.
3. Doebling SW, Farrar CR, Prime MB. A Summary Review of Vibration-Based Damage Identification Methods. *The Shock and Vibration Digest* 1998; **30**:91–105.
4. Kołakowski P, Mujica LE, Vehí J. Two Approaches to Structural Damage Identification: Model Updating vs. Soft Computing. *Journal of Intelligent Material Systems and Structures* 2006; **17**:63–79.
5. Fanning PJ, Carden EP. Experimentally validated added mass identification algorithm based on frequency response functions. *Journal of Engineering Mechanics* 2004; **130**(9):1045–1051.
6. Ge M, Lui EM. Structural damage identification using system dynamic properties. *Computers and Structures* 2005; **83**(27):2185–2196.
7. Zhang Q, Jankowski Ł, Duan Z. Identification of coexistent load and damage. *Structural and Multidisciplinary Optimization*; in press. doi 10.1007/s00158-009-0421-1.
8. Ostachowicz W, Krawczuk M, Cartmell M. The location of a concentrated mass on rectangular plates from measurements of natural vibrations. *Computers and Structures* 2002; **80**(16–17):1419–1428.
9. Mujica Delgado LE. *A hybrid approach of knowledge-based reasoning for structural assessment*. Ph.D. thesis, University of Girona, 2006.
10. Le Riche R, Gualandris D, Thomas JJ, Hemez F. Neural identification of non-linear dynamic structures. *Journal of Sound and Vibration* 2001; **248**(2):247–265.
11. Link M, Stöhr S, Weiland M. Identification of Structural Property Degradations by Computational Model Updating. *Key Engineering Materials* 2007; **347**:19–34.
12. Link M, Weiland M, Seckert Th. Computational Model Updating for Damage Identification in the Time Domain. Proc. of the International Conference on Noise and Vibration Engineering (ISMA). September 15-17, 2008, Leuven, Belgium.
13. de Lautour OR, Omenzetter P. Nearest neighbor and learning vector quantization classification for damage detection using time series analysis. *Structural Control and Health Monitoring* in press; DOI: 10.1002/stc.335
14. Faravelli L, Casciati S. Structural damage detection and localization by response change diagnosis. *Progress in Structural Engineering and Materials* 2004; **6**:104–115.
15. Casciati F, Casciati S. Structural health monitoring by Lyapunov exponents of non-linear time series. *Structural Control and Health Monitoring* 2006; **13**:132–146.
16. Holnicki-Szulc J (ed). *Smart Technologies for Safety Engineering*. John Wiley & Sons, 2008.
17. Holnicki-Szulc J, Gierliński JT. *Structural Analysis, Design and Control by the Virtual Distortion Method*. John Wiley & Sons, 1995.
18. Kołakowski P, Wikło M, Holnicki-Szulc J. The virtual distortion method — a versatile reanalysis tool for structures and systems. *Structural and Multidisciplinary Optimization* 2008; **36**(3):217–234.
19. Haftka RT, Gürdal Z. *Elements of structural optimization* (3rd edn). Kluwer Publishers, 1992.
20. Kleiber M, Antunez H, Kowalczyk P. *Parameter Sensitivity in Nonlinear Mechanics: Theory and Finite Element Computations*. John Wiley & Sons, 1997.
21. Papadimitriou DI, Giannakoglou KC. Aerodynamic Shape Optimization Using First and Second Order Adjoint and Direct Approaches. *Archives of Computational Methods in Engineering* 2008; **15**(4):447–488.
22. Suwała G, Jankowski Ł. Model-free identification of added mass. 8th World Congress on Structural and Multidisciplinary Optimization. June 1-5, 2009, Lisbon, Portugal.
23. Kress R. *Linear integral equations*. Springer: New York, 1989.
24. Nocedal J, Wright SJ. *Numerical optimization* (2nd edn). Springer, 1999.
25. Hansen PC. Deconvolution and regularization with Toeplitz matrices. *Numerical Algorithms* 2002; **29**(4):323–378.
26. Dahlquist G, Björck Å. *Numerical Methods in Scientific Computing*, vol. 1. SIAM: Philadelphia, 2008.